

# Enhancement of Zero Resistance Temperature above 90 K and Hole Distribution in $(\text{Hg}_{0.5}\text{Pb}_{0.5})\text{Sr}_2(\text{Ca}_{0.7}\text{Y}_{0.3})\text{Cu}_2\text{O}_{7-\delta}$ via Chemical Substitution of Ba into Sr Sites

R. S. Liu,<sup>\*,†</sup> J. M. Chen,<sup>‡</sup> and D. S. Shy<sup>§</sup>

Department of Chemistry, National Taiwan University, Taipei, Taiwan, ROC, Synchrotron Radiation Research Center, Hsinchu, Taiwan, ROC, and Materials Research Laboratories, Industrial Technology Research Institute, Hsinchu, Taiwan, ROC

Received September 12, 1996<sup>⊗</sup>

A significant enhancement of zero resistance temperature [ $T_{c(\text{zero})}$ ] from 78 K for  $x = 0$  to 92.5 K for  $x = 0.2$  in the series  $(\text{Hg}_{0.5}\text{Pb}_{0.5})(\text{Sr}_{2-x}\text{Ba}_x)(\text{Ca}_{0.7}\text{Y}_{0.3})\text{Cu}_2\text{O}_{7-\delta}$  compounds has been found. On the basis of the O K-edge X-ray-absorption near-edge structure (XANES) spectra for the series of  $(\text{Hg}_{0.5}\text{Pb}_{0.5})(\text{Sr}_{2-x}\text{Ba}_x)(\text{Ca}_{0.7}\text{Y}_{0.3})\text{Cu}_2\text{O}_{7-\delta}$  samples with  $x = 0-0.5$ , the chemical substitution of  $\text{Ba}^{2+}$  for  $\text{Sr}^{2+}$  gives rise to a decrease in the O 2p hole concentration within the out-of-plane oxygen sites, while that within the in-plane  $\text{CuO}_2$  layers remains almost unchanged for  $0 \leq x \leq 0.2$ . This indicates that the out-of-plane oxygen may play an important role in controlling the increase of  $T_{c(\text{zero})}$  up to the maximum value of 92.5 K.

## Introduction

A new homologous series of mercury-based superconducting  $\text{HgBa}_2\text{Ca}_{n-1}\text{Cu}_n\text{O}_{2n+2+\delta}$  ( $n = 1, 2, 3, 4$ ) compounds have been discovered<sup>1-3</sup> and the highest superconducting transition temperature ( $T_c$ ) now reaches to 134 K for the compound with  $n = 3$ . However, there remain some problems related to chemical stability. For example, an inert atmosphere is necessary during the preparation and after the preparation. On this account, a lot of attention has been focused on the investigation of barium-free mercury-based superconducting cuprates. Up to now, many Sr-based superconductors such as  $(\text{Hg}_{0.5}\text{M}_{0.5})\text{Sr}_2(\text{Ca}_{1-x}\text{Y}_x)\text{Cu}_2\text{O}_{7-\delta}$  ( $\text{M} = \text{Tl}, \text{Pb}, \text{Bi}, \text{Mo}, \text{Re}$ )<sup>4</sup> with zero resistance temperatures [ $T_{c(\text{zero})}$ ] of around 70–83 K have been found to be quite stable under open air. These new high- $T_c$  superconducting systems have a space group of  $P4/mmm$  with a tetragonal unit cell of  $a \sim 3.8 \text{ \AA}$  and  $c \sim 12 \text{ \AA}$ . The crystal structure of  $(\text{Hg}_{0.5}\text{M}_{0.5})\text{Sr}_2(\text{Ca}_{1-x}\text{Y}_x)\text{Cu}_2\text{O}_{7-\delta}$ , as illustrated in Figure 1, is similar to that of  $\text{HgBa}_2\text{CaCu}_2\text{O}_{6+\delta}$  but with some Hg replaced by M in the rock-salt layers, Ba totally replaced by Sr, and Ca partially replaced by Y.<sup>6</sup> The aim of the present research is to develop a Hg-containing Sr-based superconducting material with  $T_{c(\text{zero})}$ 's greater than 90 K that can be cooled to and easily maintained at the desired superconducting condition using the relatively less expensive liquid nitrogen. Here, we demonstrate an effective chemical substitution of the Ba ions into the Sr sites yielding a series of materials with the formula  $(\text{Hg}_{0.5}\text{Pb}_{0.5})$

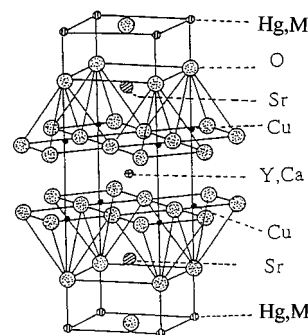


**Figure 1.** Idealized crystallographic structures of  $(\text{Hg}_{0.5}\text{M}_{0.5})(\text{Sr}_{2-x}\text{Ba}_x)(\text{Ca}_{0.7}\text{Y}_{0.3})\text{Cu}_2\text{O}_{7-\delta}$ . ( $\text{M} = \text{Tl}, \text{Pb}, \text{Bi}, \text{Mo}, \text{Re}$ .)

$(\text{Sr}_{2-x}\text{Ba}_x)(\text{Ca}_{0.7}\text{Y}_{0.3})\text{Cu}_2\text{O}_{7-\delta}$  with an enhanced  $T_{c(\text{zero})}$  from 78 K for  $x = 0$  to 90 K for  $x = 0.2$ .

To date, the precise mechanism of high-temperature superconductivity has not been delineated. A precise knowledge of the electronic structure of cuprate superconductors is an important step toward the comprehensive understanding of the origin of high- $T_c$  superconductivity. Therefore, direct experimental information on the electronic structure of these compounds is of great importance. It is a general consensus that strong hybridization of Cu-3d and O-2p wave functions places hole states on the oxygen sites in the p-type high- $T_c$  cuprate superconductors. Moreover, there are generally several non-equivalent oxygen sites, such as in-plane  $\text{CuO}_2$  layers, apical oxygen sites, etc., in the cuprate superconductors. It is therefore expected that the O K-edge X-ray absorption spectrum shows multiple pre-edge peaks due to different oxygen environments. It is important to understand the hole distribution among different oxygen sites and their role in superconductivity. In this study, O K-edge and Cu L<sub>23</sub>-edge X-ray absorption measurements were applied to probe the changes in the electronic structure of Hg-containing Sr-based  $(\text{Hg}_{0.5}\text{Pb}_{0.5})(\text{Sr}_{2-x}\text{Ba}_x)(\text{Ca}_{0.7}\text{Y}_{0.3})\text{Cu}_2\text{O}_{7-\delta}$  compounds from  $x = 0$  to 0.5.

## Experimental Section

High-purity powders of PbO, HgO, SrO<sub>2</sub>, BaO<sub>2</sub>, CaO, Y<sub>2</sub>O<sub>3</sub>, and CuO were weighted in the appropriate proportions to form nominal compositions of  $(\text{Hg}_{0.5}\text{Pb}_{0.5})(\text{Sr}_{2-x}\text{Ba}_x)(\text{Ca}_{0.7}\text{Y}_{0.3})\text{Cu}_2\text{O}_{7-\delta}$ . The powders were mixed with a mortar and pestle and then pressed into pellets (10

<sup>†</sup> National Taiwan University.

<sup>‡</sup> Synchrotron Radiation Research Center.

<sup>§</sup> Industrial Technology Research Institute.

<sup>⊗</sup> Abstract published in *Advance ACS Abstracts*, March 1, 1997.

- (1) Putilin, S. N.; Antipov, E. V.; Chmaissem, O.; Marezio, M. *Nature* **1993**, *362*, 226.
- (2) Schilling, A.; Cantoni, M.; Guo, J. D.; Ott, H. R. *Nature* **1993**, *363*, 56.
- (3) Putilin, S. N.; Antipov, E. V.; Marezio, M. *Physica C* **1993**, *212*, 226.
- (4) Liu, R. S.; Hu, S. F.; Jefferson, D. A.; Edwards, P. P.; Hunneyball, P. D. *Physica C* **1993**, *205*, 206.
- (5) Hu, S. F.; Jefferson, D. A.; Liu, R. S.; Edwards, P. P. *J. Solid State Chem.* **1993**, *103*, 280.
- (6) Liu, R. S.; Hu, S. F.; Chen, D. H.; Shy, D. S.; Jefferson, D. A. *Physica C* **1994**, *222*, 13.
- (7) Pelloquin, D.; Hervieu, M.; Michel, C.; Van Tendeloo, G.; Maigan, A.; Raveau, B. *Physica C* **1993**, *216*, 257.
- (8) Hahakura, S.; Shimoyama, J.; Shiino, O.; Kishio, K. *Physica C* **1994**, *233*, 1.

mm in diameter and 3 mm in thickness) under a pressure of 5 ton/cm<sup>2</sup>. The pellets were wrapped in gold foil to prevent the loss of lead as well as mercury and a possible reaction with quartz at elevated temperatures; they were then encapsulated in an evacuated ( $\sim 10^{-4}$  Torr) quartz tube. Subsequently, the samples were heated inside a tube furnace at a heating rate of 10 °C/min up to 970 °C for 24 h and then cooled down to room temperature at a cooling rate of 2 °C/min. After the heat treatment, all of the samples showed a black coloration.

X-ray diffraction (XRD) analyses were performed with a Philips PW 1820 X-ray diffractometer using the Ni-filtered Cu K $\alpha$  radiation. The sampling interval was 0.02 degree in  $2\theta$ , and the accumulation time was 10 s per step. The data were refined with the Rietveld analysis computer program DBWS-9006PC provided by Wiles and Young<sup>9</sup> to obtain the lattice constants. A standard four-probe method was used for electrical resistance measurements. The electrical contacts to the sample were made by fine copper wires with conductive silver paint; the applied current was 1 mA. Low-field magnetization data were taken from a superconducting quantum interference device (SQUID) magnetometer (Quantum Design). The X-ray absorption measurements were performed with the 6-m high-energy spherical grating monochromator (HSGM) beamline of the Synchrotron Radiation Research Center (SRRC) in Taiwan. The X-ray-fluorescence yield spectra were recorded with a microchannel plate (MCP) detector.<sup>10</sup> This detector consists of a dual set of MCPs with an electrically isolated grid mounted in front of them. For X-ray fluorescence yield detection, the grid was set to a voltage of 100 V while the front ends of the MCPs were set to -2000 V and the rear ends to -200 V. The grid bias insured that positive ions would not be detected while the MCP bias insured that no electrons were detected. The MCP detector was located  $\sim 2$  cm from the sample and oriented parallel to the sample surface. Photons were incident at an angle of 45° with respect to the sample normal. The incident photon flux ( $I_0$ ) was monitored simultaneously by a Ni mesh located after the exit slit of the monochromator. All of the absorption spectra were normalized to  $I_0$ . The photon energies were calibrated within an accuracy of  $\sim 0.1$  eV by using the known O K-edge and Cu L-edge absorption peaks of CuO compound. The energy resolution of the monochromator was set to  $\sim 0.22$  and  $\sim 0.45$  eV for the O K-edge and Cu L-edge absorption measurements. All the measurements were carried out at room temperature.

## Results and Discussion

The series of XRD spectra of the samples (Hg<sub>0.5</sub>Pb<sub>0.5</sub>)-(Sr<sub>2-x</sub>Ba<sub>x</sub>)(Ca<sub>0.7</sub>Y<sub>0.3</sub>)Cu<sub>2</sub>O<sub>7- $\delta$</sub>  with  $x$  varying from 0 to 0.6 are shown in Figure 2. When  $x$  is between 0 and 0.3, the compounds are nearly single phase and their spectra could be fitted to the structural model as shown in Figure 1 by assuming the Ba<sup>2+</sup> replacing Sr<sup>2+</sup> sites and the space group  $P4/mmm$  (with a tetragonal unit cell of  $a \sim 3.8$  Å and  $c \sim 12$  Å). When the value of  $x$  exceeds 0.3, the amount of an unidentified impurity phase (as denoted by "x" in Figure 2) increases.

In Figure 3, parts a and b, we show the variation of the lattice constants of  $c$  and  $a$ , respectively, as a function of  $x$  in the (Hg<sub>0.5</sub>Pb<sub>0.5</sub>)-(Sr<sub>2-x</sub>Ba<sub>x</sub>)(Ca<sub>0.7</sub>Y<sub>0.3</sub>)Cu<sub>2</sub>O<sub>7- $\delta$</sub>  series. The  $c$  lattice constant increased from 12.0077(4) Å for  $x = 0$  to 12.096(8) Å for  $x = 0.6$ , corresponding to a 0.85% increase. Moreover, the  $a$  lattice constant increased from 3.8124(1) Å for  $x = 0$  to 3.8266(1) Å for  $x = 0.6$ , representing an increase of 0.37%. These increases arise from the gradual substitution of the larger Ba<sup>2+</sup> ions [1.47 Å for coordination number (CN) of 9] into the smaller Sr<sup>2+</sup> [1.31 Å for coordination number (CN) of 9] sites.<sup>11</sup>

In Figure 4 we show the temperature dependence of the normalized resistance for the series of samples (Hg<sub>0.5</sub>Pb<sub>0.5</sub>)-(Sr<sub>2-x</sub>Ba<sub>x</sub>)(Ca<sub>0.7</sub>Y<sub>0.3</sub>)Cu<sub>2</sub>O<sub>7- $\delta$</sub> . Figure 5 is a plot of the zero resistance temperature [ $T_{(c,zero)}$ ] deduced from Figure 4 as a function of the value  $x$ . Figures 4 and 5 indicate that the

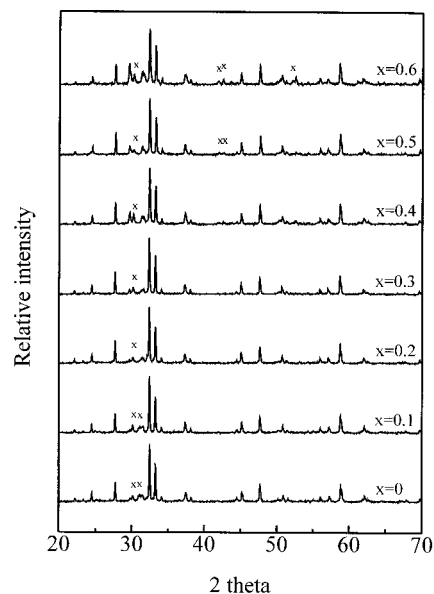


**Figure 2.** Series XRD spectra of the samples (Hg<sub>0.5</sub>Pb<sub>0.5</sub>)-(Sr<sub>2-x</sub>Ba<sub>x</sub>)-(Ca<sub>0.7</sub>Y<sub>0.3</sub>)Cu<sub>2</sub>O<sub>7- $\delta$</sub>  with  $x$  varying from 0 to 0.6.

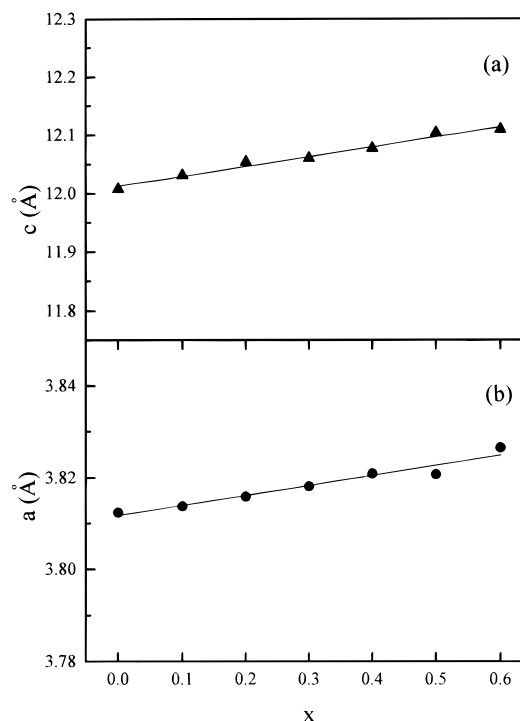


**Figure 3.** Variation of lattice constants of (a)  $c$  and (b)  $a$  as a function of  $x$  in (Hg<sub>0.5</sub>Pb<sub>0.5</sub>)-(Sr<sub>2-x</sub>Ba<sub>x</sub>)-(Ca<sub>0.7</sub>Y<sub>0.3</sub>)Cu<sub>2</sub>O<sub>7- $\delta$</sub> .

$T_{(c,zero)}$ 's for the sample with  $x = 0$  was 79 K. As Ba<sup>2+</sup> ions were added to replace the Sr<sup>2+</sup> ions (i.e., when  $x$  became nonzero), the  $T_{(c,zero)}$ 's increased and went through a maximum of 92.5 K at  $x = 0.2$  and then gradually decreased when  $x$  became greater than 0.2. However, for  $x > 0.2$ , the superconducting transition temperature became broader, which may be due to the increase in the amount of the impurity phase (as shown in Figure 2) and nonoptimal hole doping (as discussed later).

In Figure 6 we show the temperature dependence of low-field magnetization (10 G, field cooled) of the powdered samples with (a)  $x = 0$  and (b)  $x = 0.2$ . The diamagnetic onset temperatures of the  $x = 0$  and 0.2 samples appear at 82 and 96 K, respectively, which are consistent with the  $T_{(midpoint)}$ 's from the electrical resistance measurement (as shown in Figure 4).

(9) Wiles, D. B.; Young, R. A. *J. Appl. Crystallogr.* **1981**, *14*, 149.

(10) Rosenberg, R. A.; Simons, J. K.; Frigo, S. P.; Tan, K.; Chen, J. M. *Rev. Sci. Instrum.* **1992**, *63*, 2193.

(11) Shannon, R. D. *Acta Crystallogr., A* **1976**, *32*, 751.

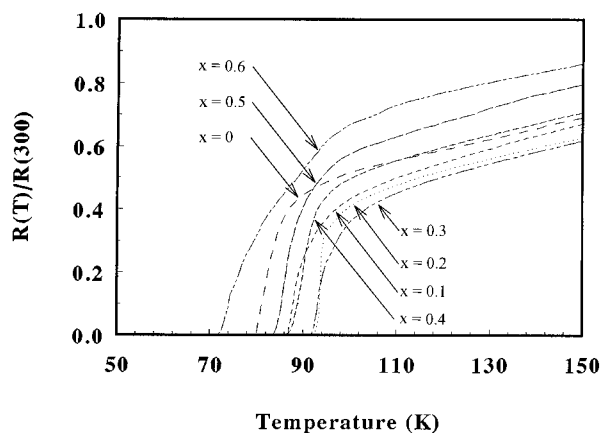


**Figure 4.** Temperature dependence of normalized resistance for the series samples  $(\text{Hg}_{0.5}\text{Pb}_{0.5})(\text{Sr}_{2-x}\text{Ba}_x)(\text{Ca}_{0.7}\text{Y}_{0.3})\text{Cu}_2\text{O}_{7-\delta}$ .

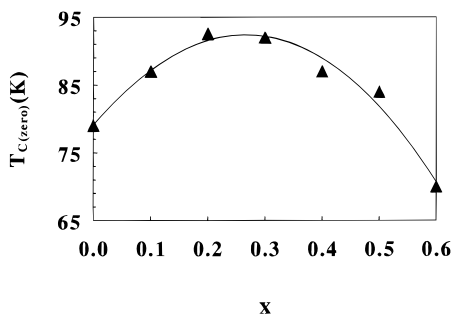


**Figure 5.** Zero resistance temperature [ $T_{c(\text{zero})}$ ] measured by electrical resistance (from Figure 4) as a function of  $x$  in  $(\text{Hg}_{0.5}\text{Pb}_{0.5})(\text{Sr}_{2-x}\text{Ba}_x)(\text{Ca}_{0.7}\text{Y}_{0.3})\text{Cu}_2\text{O}_{7-\delta}$ .

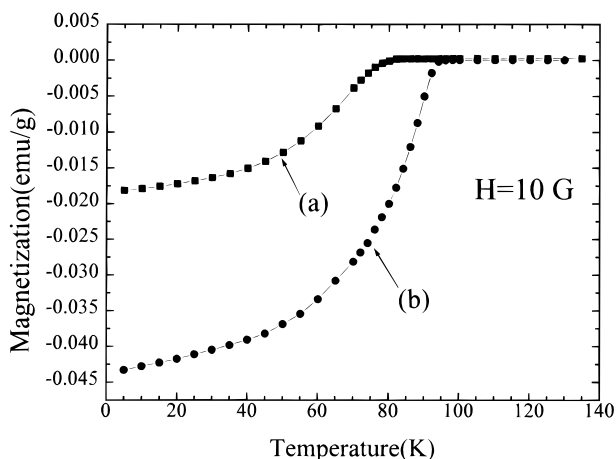


**Figure 6.** Temperature dependence of low-field magnetization (10 G, field cooled) of the powdered samples with (a)  $x = 0$  and (b)  $x = 0.2$  in  $(\text{Hg}_{0.5}\text{Pb}_{0.5})(\text{Sr}_{2-x}\text{Ba}_x)(\text{Ca}_{0.7}\text{Y}_{0.3})\text{Cu}_2\text{O}_{7-\delta}$ .

Moreover, the superconducting volume fractions of the  $x = 0$  and  $x = 0.2$  samples are around 15.4% and 36.8%, respectively, at 5 K of full diamagnetism ( $-1/4\pi$ ). The results reveal that the  $\sim 20\%$  Ba ions substituted in the Sr sites in  $(\text{Hg}_{0.5}\text{Pb}_{0.5})(\text{Sr}_{2-x}\text{Ba}_x)(\text{Ca}_{0.7}\text{Y}_{0.3})\text{Cu}_2\text{O}_{7-\delta}$  give rise to an increase in both  $T_c$  and superconducting volume fraction.

In Figure 7 we show the O K-edge X-ray-absorption near-edge structure (XANES) spectra for the series of  $(\text{Hg}_{0.5}\text{Pb}_{0.5})(\text{Sr}_{2-x}\text{Ba}_x)(\text{Ca}_{0.7}\text{Y}_{0.3})\text{Cu}_2\text{O}_{7-\delta}$  samples with  $x = 0-0.5$  in the energy range 525–555 eV obtained with a bulk-sensitive total X-ray fluorescence yield technique. The O K-edge X-ray absorption spectrum for the sample with  $x = 0$ , as shown in Figure 7, mainly consists of a peak at 529–530 eV with a shoulder at  $\sim 528.3$  eV, and a broad peak at  $\sim 537$  eV. On the

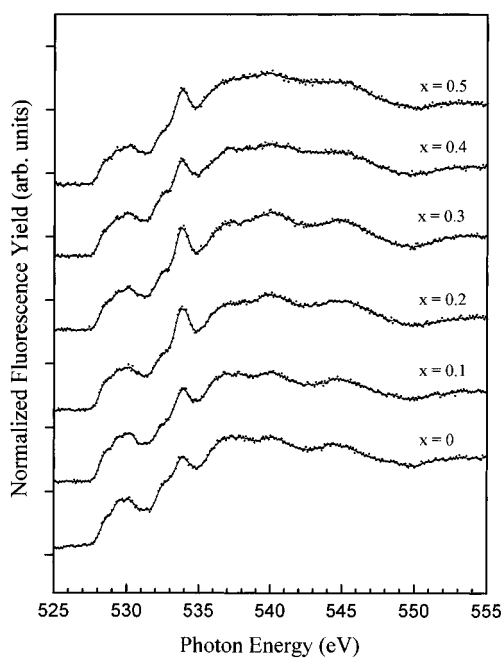


**Figure 7.** O K-edge X-ray-absorption near-edge structure (XANES) spectra for the series of  $(\text{Hg}_{0.5}\text{Pb}_{0.5})(\text{Sr}_{2-x}\text{Ba}_x)(\text{Ca}_{0.7}\text{Y}_{0.3})\text{Cu}_2\text{O}_{7-\delta}$  samples with  $x = 0-0.5$  by measuring the total X-ray fluorescence yield. These spectra have been normalized to have the same height at the main peak of  $\sim 537$  eV.

basis of the inverse photoemission studies, the empty d states of Ca, Y, and Sr are all located at about 5–10 eV above the Fermi level.<sup>12</sup> Therefore, the absorption peak at  $\sim 537$  eV may be due to the transitions from O 1s electrons to these empty d states hybridized with O 2p states. The O K-edge absorption spectra in Figure 7 were normalized to have the same height at the main peak of  $\sim 537$  eV.

In a recent investigation on the electronic structure of the Hg-based  $\text{HgBa}_2\text{Ca}_{n-1}\text{Cu}_n\text{O}_{2n+2+\delta}$  compounds for  $n \leq 3$ , Pellegrin *et al.*<sup>13</sup> have assigned the low-energy pre-edge peak at  $\sim 528.3$  eV to O 2p hole states within the  $\text{CuO}_2$  planes. This assignment was supported by the polarization-dependent X-ray absorption measurements on single-crystal  $\text{HgBa}_2\text{Ca}_3\text{Cu}_4\text{O}_{10+\delta}$ .<sup>13</sup> In addition, on the basis of the X-ray photoemission spectroscopy (XPS) studies on the O 1s core levels of epitaxial  $\text{HgBa}_2\text{CaCu}_2\text{O}_{6+\delta}$  films, the O 1s binding energy in the  $\text{CuO}_2$  planes is smaller than that in the BaO layers.<sup>14</sup> The structural arrangement of  $(\text{Hg}_{0.5}\text{Pb}_{0.5})(\text{Sr}_{2-x}\text{Ba}_x)(\text{Ca}_{0.7}\text{Y}_{0.3})\text{Cu}_2\text{O}_{7-\delta}$  is similar to that of  $\text{HgBa}_2\text{CaCu}_2\text{O}_{6+\delta}$ . We therefore adopt the same scheme in the assignment of the present O 1s pre-edge structures. In analogy to results from other hole-doped cuprate superconductors,<sup>13,15,16</sup> the pre-edge peak at  $\sim 528.3$  eV in Figure 7 for the series of  $(\text{Hg}_{0.5}\text{Pb}_{0.5})(\text{Sr}_{2-x}\text{Ba}_x)(\text{Ca}_{0.7}\text{Y}_{0.3})\text{Cu}_2\text{O}_{7-\delta}$  samples ( $x = 0-0.5$ ) can be ascribed to excitations of O 1s electrons to O 2p hole states located in the in-plane  $\text{CuO}_2$  layers. The peak at 529–530 eV is more difficult to characterize. One possible contribution to this peak could be due to transitions to the O 2p hole states within the out-of-plane oxygen sites including the SrO and HgO planes.<sup>13</sup> However, another possible

- (12) Meyer III, H. M.; Wagnener, T. J.; Weaver, J. H.; Ginley, D. S. *Phys. Rev. B* **1989**, *39*, 7243.
- (13) Pellegrin, E.; Fink, J.; Chen, C. T.; Xiong, Q.; Lin, Q. M.; Chu, C. W. *Phys. Rev. B* **1996**, *53*, 2767.
- (14) Vasquez, P.; Rupp, M.; Gupa, A.; Tsuei, C. C. *Phys. Rev. B* **1995**, *51*, 15657.
- (15) Fink, J.; Nucker, N.; Pellegrin, E.; Romberg, H.; Alexander, M.; Künfer, M. *J. Electron Spectrosc. Relat. Phenom.* **1994**, *66*, 395.
- (16) Mante, G.; Schmalz, Th.; Manzke, R.; Skibowski, M.; Alexander, M.; Fink, J. *Surf. Sci.* **1992**, *269/270*, 1071.

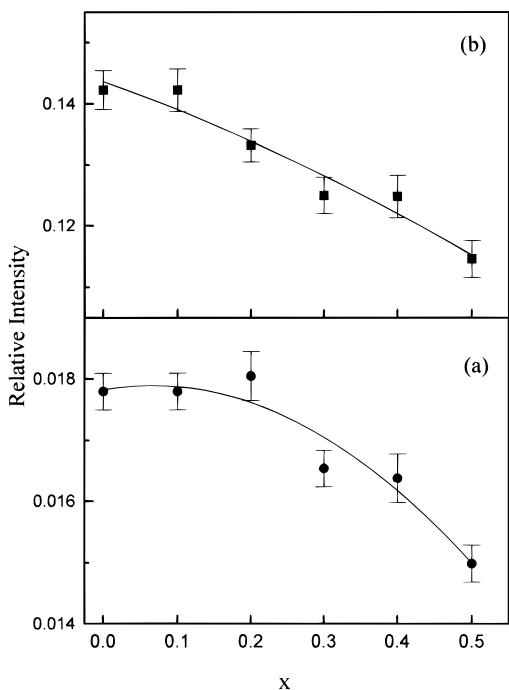


**Figure 8.** Dependence on the Ba content  $x$  in  $(\text{Hg}_{0.5}\text{Pb}_{0.5})\text{-(Sr}_{2-x}\text{Ba}_x)(\text{Ca}_{0.7}\text{Y}_{0.3})\text{Cu}_2\text{O}_{7-\delta}$  of the intensity of O 2p hole states originating from the (a) in-plane  $\text{CuO}_2$  layers and (b) out-of-plane oxygen sites. The curves are drawn as a guide for the eyes.

final state associated with the transition at 529–530 eV is the upper Hubbard band (UHB) with predominantly Cu 3d character hybridized with the O 2p states. Because of strong correlation on the copper sites in the cuprate compounds, such a band has always been assumed to exist.<sup>17</sup> Therefore, the broad peak at 529–530 eV may be due to a superposition of unoccupied O 2p states originated from the SrO and HgO layers and the upper Hubbard band related to the  $\text{CuO}_2$  planes.

The O 1s absorption features shown in Figure 7 were analyzed by fitting Gaussian functions to each spectrum. In Figure 8 the integrated intensity of the pre-edge peaks, normalized against the intensity of the main peak at  $\sim 537$  eV, is plotted as a function of compositional parameter  $x$  in  $(\text{Hg}_{0.5}\text{Pb}_{0.5})\text{-(Sr}_{2-x}\text{Ba}_x)(\text{Ca}_{0.7}\text{Y}_{0.3})\text{Cu}_2\text{O}_{7-\delta}$ . It can be seen from Figure 8a that the intensity of the pre-edge peak at  $\sim 528.3$  eV originating from the  $\text{CuO}_2$  planes remains almost unchanged for  $0 \leq x \leq 0.2$  and then decreases for  $x > 0.2$ . Conversely, the peak at 529–530 eV decreases monotonically in intensity as the Ba doping increases, as is shown in Figure 8b. This decrease may indicate that the hole concentration within the out-of-plane oxygen sites decreases with increasing Ba doping.

Several experiments and theories suggest that out-of-plane oxygen can play a relevant role in superconductivity.<sup>18–20</sup> Ohta *et al.* found a correlation between the superconducting transition temperature,  $T_c$ , and the energy difference between apical O  $2p_z$  states and O  $2p_{xy}$  states.<sup>21</sup> Also Di Castro *et al.* have explained the suppression of  $T_c$  above a certain dopant concentration by the occupancy of holes on Cu  $3d_{3z^2-r^2}$  and apical O  $2p_z$  hybrids.<sup>22</sup> Our data give evidence in support of

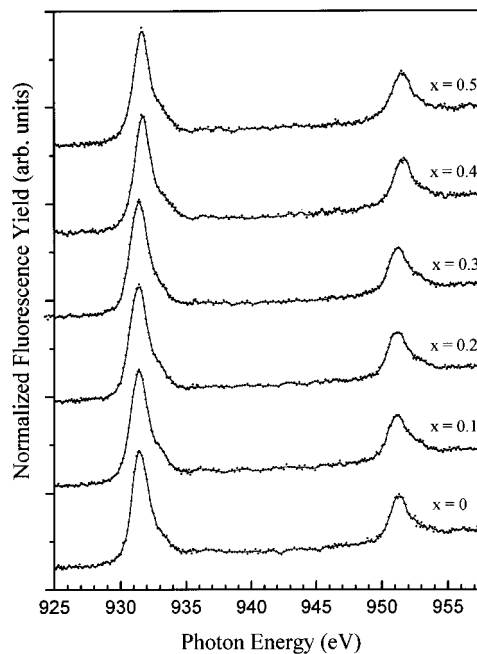


**Figure 9.** Cu L-edge X-ray-absorption near-edge structure X-ray fluorescence yield spectra for the series of  $(\text{Hg}_{0.5}\text{Pb}_{0.5})\text{-(Sr}_{2-x}\text{Ba}_x)(\text{Ca}_{0.7}\text{Y}_{0.3})\text{Cu}_2\text{O}_{7-\delta}$  samples with  $x = 0-0.5$ .

this hypothesis. As shown in Figure 8, the progressive decrease in the out-of-plane O 2p hole states with increasing the Ba concentration is accompanied by an increase in  $T_c$  for  $0 \leq x \leq 0.2$ , indicating that the covalent mixing of the out-of-plane oxygen may have a negative influence on the superconducting in  $(\text{Hg}_{0.5}\text{Pb}_{0.5})\text{-(Sr}_{2-x}\text{Ba}_x)(\text{Ca}_{0.7}\text{Y}_{0.3})\text{Cu}_2\text{O}_{7-\delta}$ . Moreover, it has been demonstrated that the concentration of O 2p holes in the  $\text{CuO}_2$  planes is strongly correlated with  $T_c$ .<sup>23</sup> Thus, the reduced hole concentration in the  $\text{CuO}_2$  planes in  $(\text{Hg}_{0.5}\text{Pb}_{0.5})\text{-(Sr}_{2-x}\text{Ba}_x)(\text{Ca}_{0.7}\text{Y}_{0.3})\text{Cu}_2\text{O}_{7-\delta}$  leads to the decrease in  $T_c$  at higher Ba doping for  $x > 0.2$ .

The peaks at 532.4 and 533.8 eV may be due to surface contamination since those peaks exhibit a greater intensity in surface-sensitive total-electron yield spectra. Existence of surface contamination has been noticed by many researchers. On the basis of their X-ray photoemission studies, Iqbal *et al.* suggested that these peaks are due to absorption of hydrides, water, and  $\text{CO}_2$  on the surface.<sup>24</sup>

In Figure 9 are shown the Cu  $L_{23}$ -edge X-ray-absorption near-edge-structure X-ray-fluorescence-yield spectra for the series of  $(\text{Hg}_{0.5}\text{Pb}_{0.5})\text{-(Sr}_{2-x}\text{Ba}_x)(\text{Ca}_{0.7}\text{Y}_{0.3})\text{Cu}_2\text{O}_{7-\delta}$  samples with  $x = 0-0.5$ . As noted from Figure 9, the Cu  $L_{23}$ -edge absorption spectra are asymmetric with two shoulders at the high-energy side of the main peaks. On the basis of curve-fitting analyses, the new features are found to center at  $\sim 933.1$  and  $\sim 952.9$  eV, respectively. The strong excitonic peaks at 931.5 and 951.3 eV are attributed to transitions from the  $\text{Cu}(2p_{3/2,1/2})3d^9\text{-O}2p^6$  ground states to the  $\text{Cu}(2p_{3/2,1/2})^{-1}3d^{10}\text{-O}2p^6$  excited states, where  $(2p_{3/2})^{-1}$  denotes a  $2p_{3/2}$  hole.<sup>25</sup> These high-energy shoulders are assigned to excitations of the  $\text{Cu}(2p_{3/2,1/2})3d^9L$  ground states to the  $\text{Cu}(2p_{3/2,1/2})^{-1}3d^{10}L$  excited states, where

(17) Vaknin, D.; Shiha, S. K.; Moneton, D. E.; Johnston, D. C.; Newsam, J. M.; Safirva, C. R.; King, H. E., Jr. *Phys. Rev. Lett.* **1987**, *58*, 2802.  
 (18) Kaldis, E.; Fischer, P.; Hewat, A. W.; Hewat, E. A.; Karpinski, J.; Rusiecki, S. *Physica C* **1989**, *159*, 668.  
 (19) Murayama, C.; Mori, N.; Yomo, S.; Takagi, H.; Uchida, S.; Tokura, Y. *Nature* **1989**, *339*, 293.  
 (20) Matsukawa, H.; Fukuyama, H. *J. Phys. Soc. Jpn.* **1990**, *59*, 1723.  
 (21) Ohta, Y.; Tohyama, T.; Maekawa, S. *Phys. Rev. B* **1991**, *43*, 2968.  
 (22) Castra, C. Di.; Feiner, L. F.; Gilli, M. *Phys. Rev. Lett.* **1991**, *66*, 3209.

(23) Krol, A.; Lin, C. S.; Soo, Y. L.; Ming, Z. H.; Kao, Y. H.; Wang, Jui H.; Qi, Min; Smith, G. C. *Phys. Rev. B* **1992**, *45*, 10051.

(24) Iqbal, Z.; Leone, E.; Chin, R.; Signorelli, A. J.; Bose, A.; Eckhardt, H. *J. Mater. Res.* **1987**, *2*, 768.

(25) Grioni, M.; Goedkoop, J. B.; Schoorl, R.; de Groot, F. M. F.; Fuggle, J. C.; Schafers, F.; Koch, E. E.; Rossi, G.; Esteva, J. M.; Kamatak, R. C. *Phys. Rev. B* **1989**, *39*, 1541.

(26) Bianconi, A.; DeSantis, M.; Di Ciccio, A.; Flank, A. M.; Fronk, A.; Fontaine, A.; Legarde, P.; Yoshida, H. K.; Kotani, A.; Marcelli, A. *Phys. Rev. B* **1988**, *38*, 7196. *Physica C* **1988**, *153-155*, 1760.

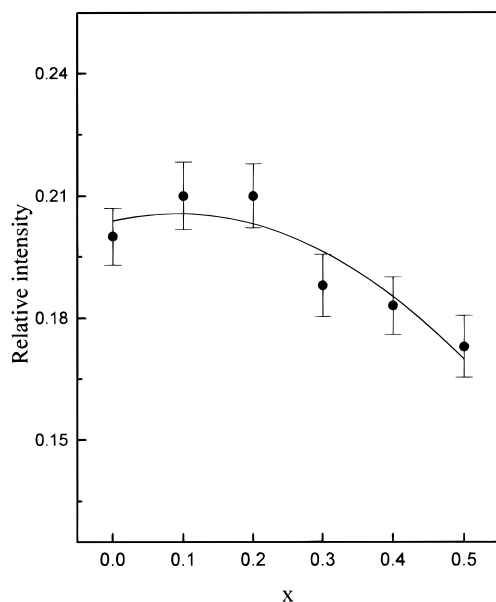


**Figure 10.** Dependence on the compositional parameter  $x$  in  $(\text{Hg}_{0.5}\text{Pb}_{0.5})(\text{Sr}_{2-x}\text{Ba}_x)(\text{Ca}_{0.7}\text{Y}_{0.3})\text{Cu}_2\text{O}_{7-\delta}$  of the normalized intensity of high-energy shoulder at  $\sim 933.1$  eV on the Cu sites. The curves are drawn as a guide for the eyes.

L denotes the O 2p ligand hole.<sup>26</sup> In Figure 10 the area under the shoulder at  $\sim 933.1$  eV, normalized against the area under the  $L_3$  peak at 931.5 eV, is displayed as function of the Ba content  $x$  in  $(\text{Hg}_{0.5}\text{Pb}_{0.5})(\text{Sr}_{2-x}\text{Ba}_x)(\text{Ca}_{0.7}\text{Y}_{0.3})\text{Cu}_2\text{O}_{7-\delta}$ . As noted from Figure 10, the normalized intensity of this high-energy shoulder keeps nearly a constant for  $0 \leq x \leq 0.2$  and decreases monotonically for  $x > 0.2$ . Because there exists only one type of Cu site in the unit cell of the  $(\text{Hg}_{0.5}\text{Pb}_{0.5})\text{Sr}_{2-x}\text{Ba}_x(\text{Ca}_{0.7}\text{Y}_{0.3})$ -

$\text{Cu}_2\text{O}_{7-\delta}$  compound (i.e., no Cu-O chains as in  $\text{YBa}_2\text{Cu}_3\text{O}_{7-\delta}$ ), these high-energy features in the Cu  $L_{23}$ -edge absorption spectra can be obviously characterized with the consequence being the O 2p hole in the  $\text{CuO}_2$  planes. Comparing Figure 10 and Figure 8a, it is found that the behavior of these high-energy shoulders correlates with that for the pre-edge peak at  $\sim 528.3$  eV in the O K-edge absorption spectra. This gives evidence in support of the suggestion that the pre-edge peak at  $\sim 528.3$  eV originates from the  $\text{CuO}_2$  planes.

In summary, a significant enhancement of zero resistance temperature [ $T_{c(\text{zero})}$ ] from 78 K for  $x = 0$  to 92.5 K for  $x = 0.2$  in the series of  $(\text{Hg}_{0.5}\text{Pb}_{0.5})(\text{Sr}_{2-x}\text{Ba}_x)(\text{Ca}_{0.7}\text{Y}_{0.3})\text{Cu}_2\text{O}_{7-\delta}$  compounds has been found. O K-edge and Cu L-edge X-ray absorption spectra of  $(\text{Hg}_{0.5}\text{Pb}_{0.5})(\text{Sr}_{2-x}\text{Ba}_x)(\text{Ca}_{0.7}\text{Y}_{0.3})\text{Cu}_2\text{O}_{7-\delta}$  with  $x = 0-0.5$  were obtained to search for the variation of electronic structure near the Fermi level related to the superconducting properties. The hole concentration in the in-plane  $\text{CuO}_2$  layers remains almost unchanged for  $0 \leq x \leq 0.2$  and then decreases for  $x > 0.2$ . Conversely, the intensity of excitation to the O 2p hole states originating from the out-of-plane oxygen sites appears to decrease monotonically with increasing Ba ion concentration. On the basis of the XANES studies, we conclude that out-of-plane oxygen plays an important factor in controlling the increase of  $T_c$  up to the maximum value of 92.5 K.

**Acknowledgment.** We would like to thank C. H. Tai and H. W. Lee at MRL/ITRI for their technical support. This research is financially supported by the National Science Council of the Republic of China under Grant No. NSC-86-2113-M-002-020.

IC9611249